ISSN 1070-3632, Russian Journal of General Chemistry, 2006, Vol. 76, No. 6, pp. 875–880. © Pleiades Publishing, Inc., 2006.
Original Russian Text © I.A. Zvereva, A.S. Isaeva, J. Choisnet, 2006, published in Zhurnal Obshchei Khimii, 2006, Vol. 76, No. 6, pp. 915–920.

Cation Distribution and Interatomic Interactions in Oxides with Heterovalent Isomorphism: XI.[1] $(La_{1-x}Ho_x)_2SrAl_2O_7$ Solid Solutions

I. A. Zvereva[a], A. S. Isaeva[a], and J. Choisnet[b]

[a] *St. Petersburg State University, Universitetskii pr. 26, St. Petersburg, 198504 Russia*
[b] *Caen University, Caen, France*

Received December 16, 2005

Abstract — Interatomic distances and distributions of rare-earth and strontium cations over two sites in the structure of $(La_{1-x}Ho_x)_2SrAl_2O_7$ solid solutions were determined by means of full-profile X-ray structural analysis. Introduction of holmium cations into the $La_2SrAl_2O_7$ oxide results in ordered distribution of Ln^{3+} cations and stabilization of the perovskite-like structure.
DOI: 10.1134/S1070363206060065

One of the directions of the development of modern chemistry is synthesis and study of compounds which can serve as a basis for creating materials with preset electrical and magnetic properties and enhanced thermal and chemical stability. The potential for practical application of such materials is extremely broad (electronics, power engineering, etc.). The functional scope of the materials can be extended by complicating their composition, in particular, by isomorphic cation substitution and obtaining solid solutions. In terms of basic science, research into the structure of solid solutions is a necessary step for revealing the composition–structure–properties relationship. At the same time, the possibilities for synthesis of solid solutions are limited by the limits of isomorphism and stability of multicomponent structures.

Here we present the results of a crystal chemical study of solid solutions obtained by the isomorphic isovalent substitution in the $La_2SrAl_2O_7$–$Ho_2SrAl_2O_7$ system. Solid solutions on the basis of rare-earth and alkaline-earth aluminates belong to promising materials for creating high-temperature ceramics with a high mechanical and thermal stability, which determines the urgency of their study.

The complex oxides $La_2SrAl_2O_7$ and $Ho_2SrAl_2O_7$ are the extreme members of the $Ln_2SrAl_2O_7$ aluminate series [2] crystallizing in the $Sr_3Ti_2O_7$ structural type, space group *I*4/*mmm* [3]. The $Ln_2SrAl_2O_7$ compounds belong to perovskite-like layered phases formed by the block principle and comprising perovskite (P) and rock salt (RS) layers alternating as PP–RS. In the structure of these compounds, the isomorphous cations Ln^{3+} and Sr^{2+} occupy 2b and 4e sites: centers of oxygen polyhedra with the coordination numbers 12 (AO_{12} octahedra) and 9 (AO_9 antiprisms) (Fig. 1). The structural peculiarities of such layered oxides consist of the possible effects of ordering of differently charged cations (rare-earth and alkaline-earth) over two nonequivalent sites, since there is a possibility for selective occupation of different polyhedra [2, 4–6]. The distribution over nonequivalent sites depends on

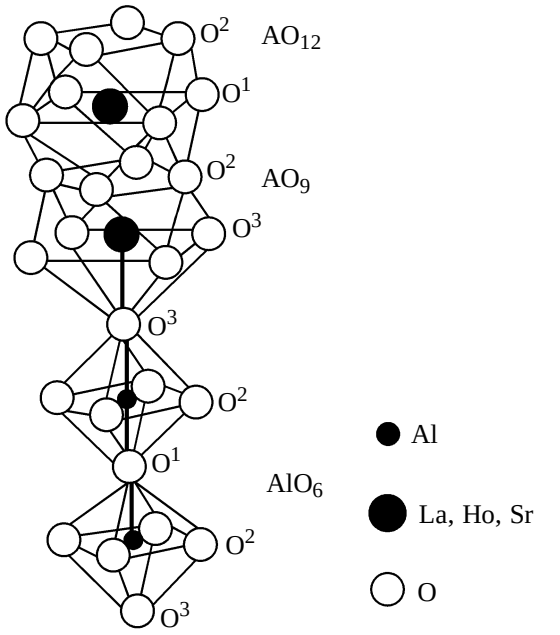

Fig. 1. AlO_6, AO_9, and AO_{12} coordination polyhedra in the structure of the $Ln_2SrAl_2O_7$ oxide.

[1] For communication X, see [1].

Table 1. Unit cell parameters a and c (Å) and volume V (Å^3), atomic coordinates (x, y, z), thermal parameters B (Å^2), structural R_F and profile R_P divergence factors (%) for $(La_{1-x}Ho_x)_2SrAl_2O_7$ solid solutions

Atom, structural site (coordinates)	Parameter	Ho content (x)									
		$x = 0$	$x = 0.2$	$x = 0.3$	$x = 0.4$	$x = 0.5$	$x = 0.6$	$x = 0.7$	$x = 0.8$	$x = 0.9$	$x = 1$
	a	3.7712(3)	3.7573	3.7501	3.7406	3.7324	3.7275	3.7224	3.7192	3.7153	3.7090(2)
	c	20.197(1)	20.125	20.065	19.986	19.901	19.830	19.733	19.634	19.547	19.448(1)
	V	287.24	284.11	282.179	279.645	277.237	275.523	273.425	271.586	269.816	267.53
La, Sr, Ho	B	0.11(2)	0.03	0.40	0.18	0.23	0.37	0.30	0.53	0.41	0.13(5)
$2b\,(0, 0, 1/2)$											
La, Sr, Ho	z	0.3186(1)	0.3184	0.3182	0.3177	0.3178	0.3181	0.3179	0.3181	0.3182	0.3180(1)
$4e\,(0, 0, z)$	B	0.45(2)	0.38	0.52	0.44	0.25	0.50	0.66	0.71	0.83	0.13(4)
Al	z	0.0933(3)	0.0994	0.0970	0.0961	0.0955	0.0965	0.0958	0.0964	0.0981	0.0943(4)
$4e\ (0, 0, z)$	B	0.20(2)	0.74	0.27	0.50	0.13	0.24	0.54	0.58	0.42	0.65(5)
O^1	B	1.24(2)	1.2	1.2	1.2	1.2	1.2	1.2	1.2	1.2	1.1(5)
$2a\,(0, 0, 0)$											
O^2	z	0.0942(4)	0.1010	0.0981	0.0983	0.0989	0.0998	0.1009	0.1020	0.1048	0.1012(4)
$8g\,(0, 1/2, z)$	B	0.77(2)	2.3	1.6	1.1	0.47	0.81	0.39	1.1	0.95	0.93(2)
O^3	z	0.1977(5)	0.1931	0.1938	0.1983	0.2012	0.1994	0.1987	0.2028	0.2046	0.207(1)
$4e\,(0, 0, z)$	B	0.6(2)	1.9	0.5	1.1	1.2	1.5	2.2	2.8	1.7	1.0(5)
	R_F	7.7	9.1	6.8	5.2	6.0	6.5	6.9	7.0	9.9	6.1
	R_P	13.9	6.9	5.6	4.0	4.8	5.2	5.1	6.0	7.4	17

Table 2. Occupancy of structural sites (AO_{12} and AO_9 polyhedra) in $(La_{0.7}Ho_{0.3})_2SrAl_2O_7$ solid solutions

Solid solutions	AO_{12}			AO_9		
	La^{+3}	Ho^{+3}	Sr^{+2}	La^{+3}	Ho^{+3}	Sr^{+2}
$La_2SrAl_2O_7$	0.73	–	0.27	1.27	–	0.73
$(La_{0.9}Ho_{0.1})_2SrAl_2O_7$	0.66	0.07	0.27	1.14	0.13	0.73
$(La_{0.8}Ho_{0.2})_2SrAl_2O_7$	0.61	0.05	0.34	1.00	0.35	0.65
$(La_{0.7}Ho_{0.3})_2SrAl_2O_7$	0.58	0.08	0.34	0.82	0.53	0.65
$(La_{0.6}Ho_{0.4})_2SrAl_2O_7$	0.53	0.10	0.37	0.67	0.70	0.63
$(La_{0.5}Ho_{0.5})_2SrAl_2O_7$	0.49	0.12	0.39	0.51	0.88	0.61
$(La_{0.4}Ho_{0.6})_2SrAl_2O_7$	0.37	0.17	0.46	0.43	1.03	0.54
$(La_{0.3}Ho_{0.7})_2SrAl_2O_7$	0.21	0.26	0.53	0.39	1.14	0.47
$(La_{0.2}Ho_{0.8})_2SrAl_2O_7$	0.12	0.31	0.57	0.28	1.29	0.43
$(La_{0.1}Ho_{0.9})_2SrAl_2O_7$	0.02	0.29	0.69	0.18	1.51	0.31
$Ho_2SrAl_2O_7$	–	0.18	0.82	–	1.82	0.18

the nature of the rare-earth element, and in the La–Ho series a transition occurs from an almost disordered distribution of La^{3+} and Sr^{2+} in $La_2SrAl_2O_7$ to ordered distribution with preferential occupation of AO_9 antiprisms by Ho^{3+} cations in $Ho_2SrAl_2O_7$ [2]. The positional ordering of differently charged cations, La^{3+}, Sr^{2+}, and Ca^{2+}, was also found also in $La_2Sr_{1-x}Ca_x \cdot Al_2O_7$ and $Nd_2Sr_{1-x}Ca_xAl_2O_7$ solid solutions [5, 6].

In this work we made use of full-profile Rietveld X-ray diffraction analysis to obtain crystal chemical data for $(La_{1-x}Ho_x)_2SrAl_2O_7$ solid solutions, including data on occupation of different polyhedra with La^{3+}, Ho^{3+}, and Sr^{2+} ions.

The results of structural calculations in the *I*4/*mmm* space group are given in Tables 1 and 2. The experi-

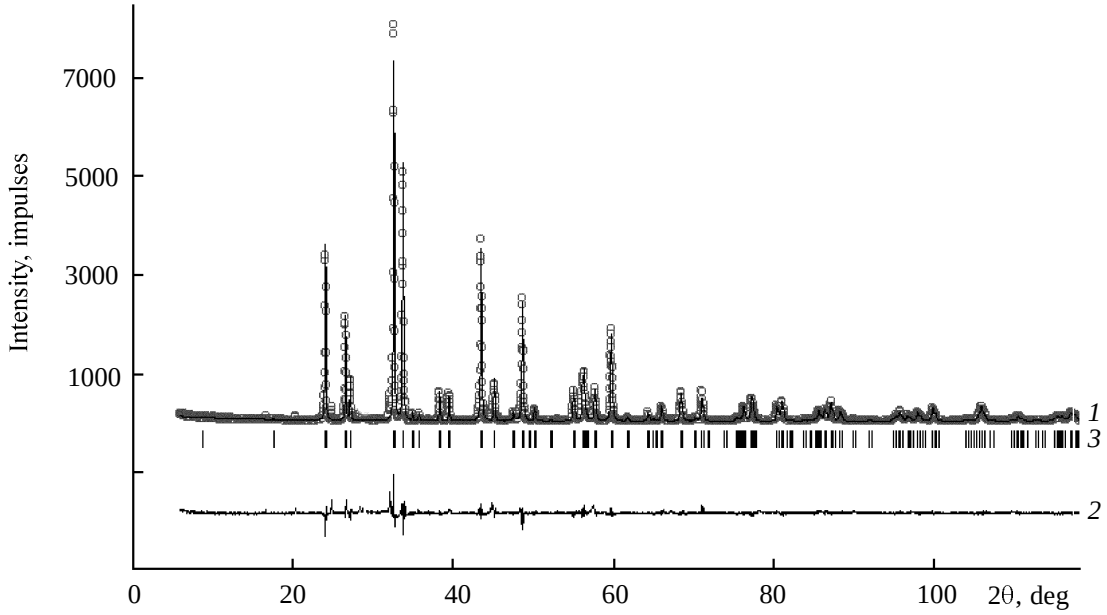

Fig. 2. (Circles) Experimental, (*1*) calculated, and (*2*) differential X-ray pattern profiles and (*3*) location of Bragg's maxima as functions of the scattering angle 2θ, for the $(La_{0.7}Ho_{0.3})_2SrAl_2O_7$ solid solution.

mental, calculated, and differential profiles of the X-ray pattern for the $(La_{0.7}Ho_{0.3})_2SrAl_2O_7$ solid solution are shown in Fig. 2. In the X-ray patterns of the solid solutions, all maxima correspond to reflexes of the $Sr_3Ti_2O_7$ structural type in which the $Ln_2SrAl_2O_7$ complex aluminates crystallize. The monotonous changes of unit cell parameters with holmium content (Fig. 3) points to the formation of a continuous series of $(La_{1-x}Ho_x)_2SrAl_2O_7$ ($0 \le x \le 1$) solid solutions. As the holmium content of the solid solution increases, the unit cell parameters and volume decrease, in parallel with the decreasing average ionic radius of the lanthanide. A similar trend is observed for the entire La–Ho series. In a number of solid solutions at $x > 0.5$, as well as in all $Ln_2SrAl_2O_7$ oxides starting from gadolinium, the a parameter decreases to a lesser extent.

The atomic coordinates expressed in period fractions remain almost invariable with varying concentration of the solid solutions. The greatest changes are characteristic of O^2 and O^3.

The calculated occupancies of two structural sites with isomorphous cations (Table 2) point to the fact that holmium cations prefer to occupy nine-coordinated sites in the $La_2SrAl_2O_7$ matrix. Therewith, lanthanum and strontium cations are expelled to AO_{12} cubic octahedra. This trend is accounted for by the fact that smaller holmium atoms {$R(La^{3+})$ 1.216, $R(Sr^{2+})$ 1.31, and $R(Ho^{3+})$ 1.072 A [7]} tend to occupy smaller AO_9 polyhedra. Figure 4 compares

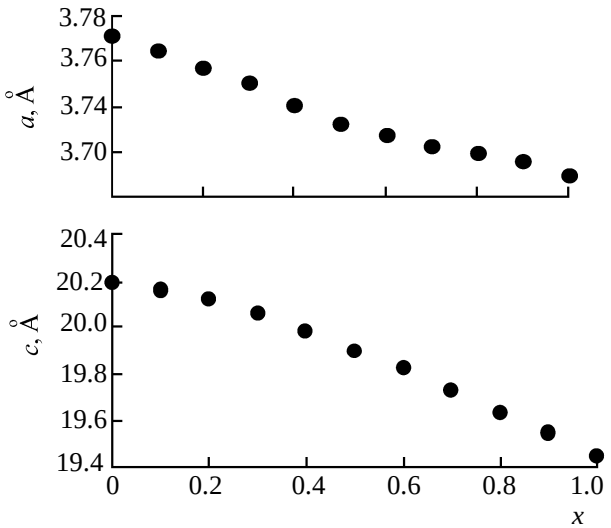

Fig. 3. Unit cell parameters *a* and *c* of $(La_{1-x}Ho_x)_2 \cdot SrAl_2O_7$ solid solutions vs. holmium content (*x*).

the occupancies of the AO_9 polyhedra located in the rock salt layer with rare-earth cations (La^{3+} and Ho^{3+}) in the solid solutions in comparison with those in oxides of the $Ln_2SrAl_2O_7$ series, as a function of the average ionic radius of a nine-coordinated rare-earth element. Such a cation distribution over two nonequivalent sites points to positional ordering of differently charged La^{3+}, Sr^{2+}, and Ho^{3+} cations not only in oxides, but also in solid solutions. This ordering enhances as the holmium content in the solid solu-

Table 3. Interatomic distances in AO_{12}, AO_9, and AlO_6 coordination polyhedra as a function of the concentration of the $(La_{1-x}Ho_x)_2SrAl_2O_7$ solid solution

Interatomic distance	Ho content (x)									
	x = 0	x = 0.2	x = 0.3	x = 0.4	x = 0.5	x = 0.6	x = 0.7	x = 0.8	x = 0.9	x = 1
					AO_{12}					
$A–O^1 \times 4$	2.667	2.657	2.652	2.645	2.639	2.636	2.632	2.630	2.627	2.623
$A–O^2 \times 8$	2.705	2.768	2.723	2.713	2.710	2.713	2.716	2.729	2.706	2.704
					AO_9					
$A–O^3 \times 1$	2.569	2.521	2.502	2.388	2.331	2.365	2.375	2.269	2.225	2.159
$A–O^3 \times 4$	2.674	2.667	2.662	2.664	2.665	2.657	2.650	2.661	2.664	2.667
$A–O^2 \times 4$	2.557	2.482	2.512	2.512	2.497	2.479	2.463	2.437	2.394	2.431
					AlO_6					
$Al–O^3 \times 1$	1.901	1.886	1.932	2.042	2.090	2.030	2.009	2.084	2.080	2.153
$Al–O^1 \times 1$	1.964	2.001	1.952	1.920	1.905	1.914	1.891	1.893	1.915	1.873
$Al–O^2 \times 4$	1.886	1.879	1.875	1.871	1.867	1.865	1.863	1.863	1.862	1.857
$Al–O_{av} \times 6$	1,902	1.901	1.897	1.915	1.910	1.901	1.892	1.904	1.907	1.903
$A–O^3–Al$	4.470	4.407	4.434	4.430	4.421	4.395	4.384	4.353	4.305	4.312
$O^3–Al–O^1–Al–O^3$	7.730	7.774	7.768	7.924	7.990	7.888	7.800	7.954	7.990	8.052

tions increases. Comparison with the oxide series shows that the tendency for La^{3+} and Sr^{2+} ordering in the solid solutions is slightly weaker. Three factors can be responsible for this phenomenon. First, the third component exerts a disordering effect: Three cations, rather than two as in oxides, are distributed over two structural sites. Second, the difference in the size of rare-earth elements and strontium plays a weaker role, since La^{3+} and Sr^{2+} are close in size. Third, rare-earth atoms in solid solutions have, on average, a smaller number of unpaired electrons, which should weaken interactions between paramagnetic atoms within the rock salt layer. In should be noted that the first and third factors should contribute more at medium solution concentrations and for oxides with the maximum spin of rare-earth atoms, e.g. Eu, Gd, and Tb.

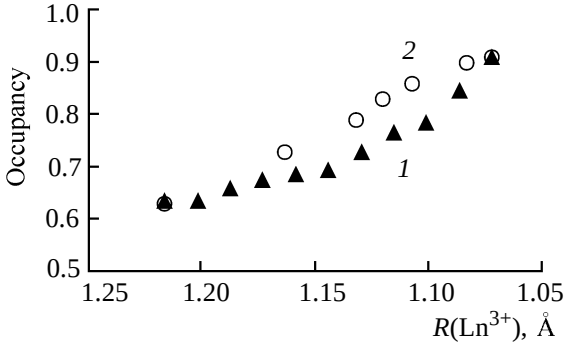

Fig. 4. Occupancy of AO_9 polyhedra with rare-earth cations in (*1*) $(La_{1-x}Ho_x)_2SrAl_2O_7$ solid solutions and (*2*) $Ln_2SrAl_2O_7$ complex oxides (Ln = La, Nd, Sm, Eu, Gd, Dy, Tb, Ho) vs. average radius of Ln^{3+} in the nine-coordinated state.

The positional ordering in the series of solid solutions substantially decreases the probability of composition fluctuations that form local regions enriched with lanthanide cations in the P layer. Such regions can destabilize the layered PP–RS structure, since they can be precursors of perovskite isolation. It is the least thermodynamically stable $La_2SrAl_2O_7$ compound with a close-to-disordered distribution, that decomposes into $LaAlO_3$ and $LaSrAlO_4$ on prolonged heating at 1000°C (100 h). As we showed in the present study, $(La_{1-x}Ho_x)_2SrAl_2O_7$ solid solutions do not decompose under the same thermodynamic conditions. Therefore, we now have evidence to show that enrichment of the RS layer with lanthanide cations results in stabilization of the layered structure, as shown previously for the $Ln_2SrAl_2O_7$ (Ln = La, Nd, Sm, Eu, Gd, Tb, Dy, Ho) oxide series [8]. It is significant that in the $La_2Sr_{1-x}Ca_xAl_2O_7$ solid solutions we studied previously, Ca^{2+} ions are fully ordered in the RS layer, which limits the existence region of the solid solutions [5].

The interatomic distances in the coordination polyhedra in $(La_{1-x}Ho_x)_2SrAl_2O_7$ solid solutions are given in Table 3. Figure 5 shows the plots of interatomic distances vs. the average radius of nine-coordinated lanthanide for the $(La_{1-x}Ho_x)_2SrAl_2O_7$ series and, for comparison, for the $Ln_2SrAl_2O_7$ series.

Examination of the curves (Fig. 5a) suggests that the solid solutions all have distorted AlO_6 octahedra. The latter are more exact to call base-shared double tetragonal pyramids. As the concentration of holmium increases, the distance between Al^{3+} and the oxygen atom located in the RS layer ($Al–O^3$) increases. At the same time, the distance between Al^{3+} and the axial O^1 atom located in the P layer ($Al–O^1$) slightly decreases. In the $La_2SrAl_2O_7$ oxide, the distance between Al^{3+} and the O^3 ion located in the RS layer almost coincides with the length of the equatorial $Al–O^2$ bond, which decreases monotonously. As the holmium content increases, the character of octahedron distortion changes: At $x = 0.3$, the bipyramid oblong inward the P layer almost transforms into a tetragonally distorted octahedron. On further increase in the holmium content, the symmetry of the oxygen surrounding of aluminum decreases again to a bipyramid flattened inward the P layer. The same trend in interatomic distances in the AlO_6 polyhedron is also observed in the $Ln_2SrAl_2O_7$ (La–Ho) series, with decreasing lanthanide radius. The average Al–O bond length in the octahedra remains almost unchanged: As $Al–O^3$ weaken, the thickness of the PP double perovskite layer ($O^3–Al–O^1–Al–O^3$) substantially increases with simultaneous decrease in the interlayer spacing ($A–O^3–Al$). This agrees with the preferential occupation of AO^{12} polyhedra with larger strontium cations. The strengthening of the $Al–O^1–Al$ bond, i.e. decreased distance between aluminum atoms, is associated with the fact that Ho^{3+} stronger polarize oxygen atomic orbitals than Sr^{2+} and La^{3+}. Therefore, the distortion of octahedra in the solid solution mainly depends on the average ionic radius of lanthanide atoms.

The trend in interatomic distances in the AO_9 antiprism (Fig. 5b) shows that, as the holmium content increases and the average ionic radius of lanthanide decreases, the length of axial (La, Ho, Sr)–O^3_{ax} bonds substantially increases, whereas the length of equatorial (La, Ho, Sr)–O^3_{eq} and (La,Ho,Sr)–O^2 bonds changes only slightly. In this case, the shortening of four $A–O^2$ bonds (by 0.13 Å) and one $A–O^3_{ax}$ bond (by 0.41 Å) in the AO_9 polyhedron correlates with the preferential occupation of AO_9 polyhedra with smaller holmium cations.

The bond lengths in the AO_{12} cubic octahedron undergo the smallest changes along the entire series of the solid solutions (eight $A–O^2$ bonds scarcely change length and four $A–O^1$ bonds shorten by 0.04 Å only). This is also in agreement with the positional ordering, since smaller holmium atoms introduced into the $La_2SrAl_2O_7$ matrix occupy cubic

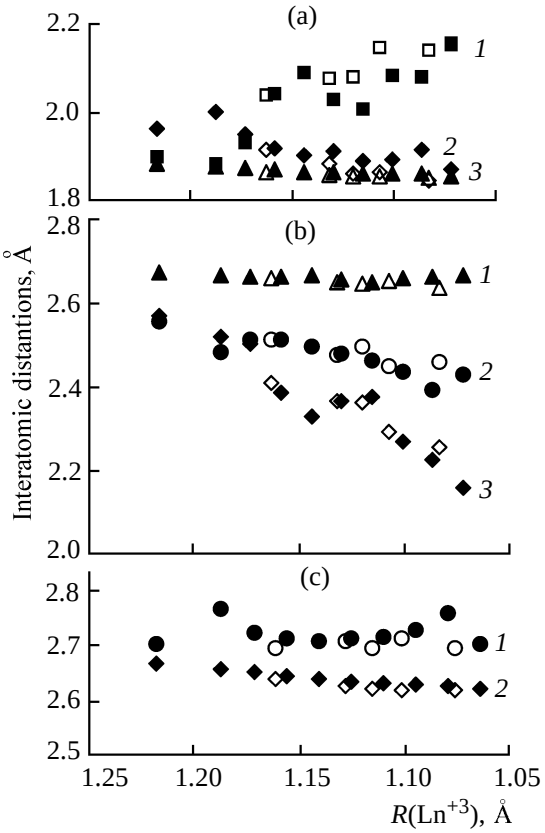

Fig. 5. Plots of interatomic distances vs. average radius of Ln^{3+} in coordination polyhedra for (black signs) $(La_{1-x}Ho_x)_2SrAl_2O_7$ solid solutions and (light signs) $Ln_2SrAl_2O_7$ oxides (Ln = La, Nd, Sm, Eu, Gd, Dy, Ho). (a) AlO_6 octahedron: (*1*) $Al–O^3$, (*2*) $Al–O^1$, and (*3*) $Al–O^2$; (b) AO_9 antiprism: (*1*) $A–O^3_{eq}$, (*2*) $A–O^2$, and (*3*) $A–O^3_{ax}$; and (c) AO_{12} octahedron: (*1*) $A–O^2$ and (*2*) $A–O^1$.

octahedra in the P layer only to a minor extent, and lanthanum and strontium atoms are close in size.

In the $Al–O_3–(Ln, Sr)$ chain linking the P and RS layers, there is bond competition which shows itself in weakening of the $Al–O^3$ bond and strengthening of the $Ln(Sr)–O^3$ bond with increasing holmium content. This fact provides evidence to show that bonds between the fragments of the layered structure and bonds within the layers strengthen, as the occupancy of the RS layers with holmium atoms increases.

Therefore, the results of our crystal chemical study of solid solutions having differently charged rare-earth and alkaline-earth cations occupying two nonequivalent common sites show that isomorphous isovalent replacement by smaller lanthanide atoms stabilizes the layered structure. This finding provides evidence for an important role the dimension factor and positional

ordering play in the structural chemical mechanism of formation of compounds with heterovalent isomorphism.

EXPERIMENTAL

The synthesis of $(La_{1-x}Ho_x)_2SrAl_2O_7$ solid solutions was performed by the standard ceramic procedure. Lanthanum and holmium oxides (Johnson Matthey) containing 99.95 and 99.99% of the main component, respectively, special purity grade 7–2 strontium carbonate (Technical Specifications 6-09-01-659-91), and finely dispersed aluminum oxide (Johnson Matthey, 99.99%, 1–15 μm) containing a certain amount of the γ modification were used. The batch prepared with the stoichiometric proportions of the starting materials, corresponding to the reaction equation given below, was thoroughly mixed, pressed into pellets 0.5 g in weight and 0.7 cm in diameter, and calcined in a Silit oven in corundum crucibles in air for 30 h at 1450°C.

$$(1 - xLn_2O_3 + xHo_2O_3 + Al_2O_3 + SrCO_3 = (Ln_{1-x}Ho_x)_2SrAl_2O_7 + CO_2.$$

The isothermal regime of heat treatment was maintained with an accuracy of ±1°C, using a TP-403 programmed temperature controller.

The thermal stability of the solid solutions was controlled under conditions of isothermal annealing at 1000°C for 100 h.

The phase composition of the calcined sampled was controlled by X-ray diffraction. The X-ray patterns were recorded on a Philips Analytical Z-ray PW-3020 diffractometer (CuK_α radiation) within the 2θ range 5°–50° at 0.05° intervals and a constant count time of 2 s. The X-ray patterns for structural calculations were recorded in the angle range 5°–110° at 0.04° intervals and constant count time of 12 s.

The unit cell parameters, atomic coordinates, interatomic distances, and site occupancies were determined in the *I*4/*mmm* space group from the full-profile of the X-ray pattern with subsequent Rietveld refinement [9] using the FULPROF program [10].

ACKNOWLEDGMENTS

The work was financially supported by the Russian Foundation for Basic Research (grant no. 04-03-32176).

REFERENCES

1. Zvereva, I.A., Smirnov, Yu.E., and Palstra, T., *Zh. Obshch. Khim.*, 2006, vol. 76, no. 3, p. 353.
2. Zvereva, I., Smirnov, Yu., Gusarov, V., Popova, V., and Choisnet, J., *Solid State Science*, 2003, vol. 5, no. 2, p. 343.
3. Ruddlesden, S.N. and Popper, P., *Acta Crystallogr.*, 1958, vol. 11, no. 1, p. 54.
4. Zvereva, I.A., Smirnov, Yu.E., Vagapov, D.A., and Choisnet, J., *Zh. Obshch. Khim.*, 2000, vol. 70, no. 12, p. 1957.
5. Zvereva, I., Smirnov, Yu., and Choisnet, J., *Int. J. Inorg. Mater.*, 2001, vol. 3, no. 1, p. 95.
6. Zvereva, I.A., Seitablaeva, S.R., and Smirnov, Yu.E., *Zh. Obshch. Khim.*, 2003, vol. 73, no. 1, p. 35.
7. Shannon, R.D., *Acta Crystallogr., Sect. A*, 1976, vol. 32, no. 5, p. 751.
8. Zvereva, I.A., Abstracts of Papers, *XV Mezhdunarodnaya konferentsiya po khimicheskoi termodinamike v Rossii* (XV Int. Conf. on Chemical Thermodynamics in Russia), Moscow, 2005, p. 186.
9. Rietveld, H., *Appl. Crystallorg.*, 1969, vol. 2, no. 1, p. 65.
10. Rodriguez-Carvajal, J.L., *Physica B*, 1992, vol. 192, no. 1, p. 55.